BLAST WAVE AND FIREBALL AFTER HYDROGEN TANK RUPTURE IN A FIRE

V. V. Molkov[1], D. M. C. Cirrone[1], V. V. Shentsov[1], W. Dery[1], W. Kim[2], and D. V. Makarov[1]

[1]Ulster University
 Hydrogen Safety Engineering and Research Centre (HySAFER)
 Newtownabbey, BT37 0NL, Northern Ireland, U.K.
e-mail: v.molkov@ulster.ac.uk

[2]Department of Mechanical Systems Engineering
 Hiroshima University
 1-4-1 Kagamiyama, Higashi-Hiroshima 739-8527, Japan

The development of computational fluid dynamics (CFD) model to simulate blast wave and fireball dynamics after high-pressure hydrogen tank rupture in a fire is described. Parametric study is performed to define the effect of submodels, numerical methods, and parameters on the convergence of the simulations and reproduction of experimental data. Experiments with initial pressure in hydrogen tank of 350 and 700 bar were used to validate the model. The effect of hydrogen combustion and tank opening on the blast wave strength is assessed. The simulated cases include instantaneous tank opening and half tank opening.

Introduction

Hydrogen-powered cars and buses are already on the roads. Statistics of accidents with CNG (compressed natural gas) vehicles shows that more than 1/3 of a total number of tank ruptures in a fire is due to pressure relief device failure. Volume of storage tanks ranges from 20 to 140 l. The risk of hydrogen-powered vehicles is above the acceptable level of 10^{-5} if the onboard storage tank has fire resistance rating below 47 min for example of London roads [1]. This accounts for nonzero probability of thermally activated pressure relief device

V. V. Molkov et al.

(TPRD) failure. The calculation of risk implies the assessment of consequences of high-pressure hydrogen tank rupture in a fire. This, in turn, requires understanding of two main hazards from a tank rupture: blast wave and fireball. To formulate innovative mitigation strategies and develop engineering solutions for safety on hydrogen vehicles, the underpinning physical phenomena should be understood first. The aim is to develop and validate a CFD model to get insights into formation and dynamics of blast wave and fireball after stand-alone tank rupture in a fire in the open. This work expands the studies performed in HySAFER previously [2–4].

Validation Experiments

USA test

The experimental data on fire test of stand-alone Type 4 hydrogen storage tank without TPRD performed by Weyandt in 2005 are published elsewhere [5–8]. The tank length was 0.84 m, diameter 0.41 m, and internal volume 72.4 l. Initial storage pressure was 34.3 MPa and temperature 300 K (1.64 kg of hydrogen). At time of rupture (after 6 min 27 s of 350 kW fire exposure), they raised to 35.7 MPa and 312.15 K, respectively. The tank was placed 0.2 m above the ground over a propane burner. Three sensors were located perpendicular to the tank axis in a straight line at distances 1.9, 4.2, and 6.5 m from the tank center. The fourth sensor was located along the tank axis at 4.2 m. The measured maximum pressure was 300, 83, and 41 kPa at 1.9, 4.2, and 6.5 m, respectively (perpendicular to the tank axis), and 64.8 kPa for the sensor at 4.2 m along the tank axis. The blast wave decayed faster along the tank axis (25 percent reduction of overpressure from 83 to 64.8 kPa at 4.2 m). The released mechanical energy was estimated as 7.33 MJ and chemical energy that contributed to the blast wave strength as 10.3 MJ [9]. The maximum reported diameter of the fireball was about 7.7 m (at time 45 ms after the tank rupture).

Japanese tests

Two fire tests were conducted in Japan on tanks with nominal pressure 70 MPa. The blast wave pressure was recorded at distance 5

V. V. Molkov et al.

261

and 10 m perpendicular to the tank axis. Fire Test 1 was conducted with a Type 4 tank of 35-liter volume. The tank ruptured after 21 min of fire exposure. The last recorded pressure in the tank was 94.54 MPa. The maximum overpressure at 5 and 10 m was 110.5 and 23.4 kPa, respectively. Fire Test 2 was conducted with a Type 3 tank of 36-liter volume. The pressure measured before the tank burst at 11 min after the fire exposure was 99.47 MPa. The maximum overpressure recorded at the probe sensors was 74.3 kPa at 5 m and 23.4 kPa at 10 m. In Test 2, the maximum overpressure at the 5-meter sensor was 30% less than in Test 1, despite the slightly bigger volume and pressure before burst. Both tests resulted in a fireball with diameter approximately 20 m.

Computational Fluid Dynamics Model and Numerical Details

The following common features of the CFD model were used in simulation of the USA test and two Japanese tests. Simulations were performed using Fluent as the computational engine. The pressure-based solver was used coupled with PISO (Pressure-Implicit with Splitting of Operators) pressure–velocity algorithm. The large eddy simulation (LES) approach was applied. The governing equations are based on the filtered conservation equations for mass, momentum, and energy in their compressible form. The ground is specified as an adiabatic no slip wall. The external nonreflecting boundary is defined as pressure outlet with zero gauge pressure. Hydrogen at pressures 350–100 bar behaves as real gas. The pressure in a starting shock is below 100 bar and thus combustion at contact surface could be considered as combustion of ideal gas. For Japanese tests accounting for the increase of pressure and temperature before burst, starting shock is 62.14 and 63.36 bar for Tests 1 and 2, respectively. The simulations were performed with ideal gas equation of state (EoS). Due to more complicated real gas EoS, the numerical solution procedure is prawn to sometimes produce untenable results avoiding averting convergence and, furthermore, increases the calculation times drastically [10].

To conserve the mechanical energy of compressed hydrogen during transition from the volume of tank with real gas (V_{real}) to the

volume of scaled tank with ideal gas used in simulations (V_{ideal}), the following formulae based on the Able–Noble equation was applied for geometrical scaling:

$$V_{\text{ideal}} = V_{\text{real}} - mb$$

where m is the mass of hydrogen and b is the co-volume constant. For the USA test with 1.64 kg of hydrogen, the cylinder size in simulations was scaled down to 68.4 cm in length and 37.7 cm in diameter. The temperature and pressure in the tank were set to 312 K and 35.7 MPa as observed in the test just before its failure.

The second-order discretization scheme was used for pressure to improve accuracy for compressible flows. The second-order upwind scheme is used for convective terms while the first order is employed for time advancement. Change to the second-order scheme for the case of constant time step did not cause any difference in the resulting pressure dynamics. The original time step adapting technique was employed to maintain a constant Courant–Friedrichs–Lewy (CFL) number, and to provide a significant saving of computational time compared to constant time step. The convergence of simulations by CFL was checked before the numerical tests were carried out.

Numerical details for USA test

The Smagorinsky–Lilly model was used for subgrid scale (SGS) turbulence modeling. To simulate the combustion and turbulence–chemistry interaction, the eddy-dissipation-concept (EDC) [11] was employed. Either detailed chemical mechanism or one-step Arrhenius chemistry for hydrogen combustion in the air can be applied. To reduce calculation time, one-step Arrhenius chemistry is applied in this study. Combustion in the fine scale is governed by the Arrhenius chemistry and for the detailed chemical mechanism case, it is integrated numerically using the ISAT (*In Situ* Adaptive Tabulation) algorithm, offering substantial reduction in run-time. The computational domain was a hemisphere of 100-meter diameter. Hexahedral mesh with the total number of control volumes (CVs) 311114 was created. To provide numerical ignition, the temperature around the tank was heated to exceed the activation energy threshold required to maintain combustion. In this specific case, a rectangular area of sizes $1.5 \times 0.7 \times 0.9$ m of volume 0.945 m^3 patched around the tank was

initialized with a temperature of 900 K and mass fraction of water vapor of 0.01. The remaining domain had pressure of 101,325 kPa and temperature of 293 K as ambient conditions.

Numerical details for Japanese tests

Two SGS turbulence model were applied in simulations of Japanese tests. All simulations were performed with the renormalization group (RNG) theory [12] and then compared to Smagorinsky–Lilly model [13]. The effect of radiation was assessed through the application of Discrete Ordinates model [14] which was found to have no practical effect on pressure. Here, instead of EDC model applied in simulating the USA test, the chemical source term was calculated through the Arrhenius reaction rate for one-step chemical reaction without calculating fine-scales as in EDC model. It is called here as finite rate chemistry (FRC) model. CFL was imposed to value 0.2. The tank volume was scaled from 35 to 23.9 l for Test 1 and from 36 to 24.6 l for Test 2. Hexahedral mesh of 147104 CVs was used. The domain is initialized with pressure equal to 101.325 kPa, temperature 282 K, and air composition. The region corresponding to the tank is initialized with hydrogen mass fraction equal to 1 and the pressure measured before burst 94.54 and 99.47 MPa for Tests 1 and 2, respectively. The temperature in the tank before burst was not measured; so, it was calculated from the Abel–Noble EoS for both the tests.

Results and Discussions

USA test

The results of CFL convergence exercise, which has to be carried out before any parametric study, are shown in Fig. 1a. It is concluded that the convergence of solution is achieved at CFL ≤ 0.1. Further simulations were performed at CFL $= 0.1$. Figure 1b shows maximum pressures in the near to the tank field in directions perpendicular to and along the tank axis. The faster shock decay with distance for tank end is due to more pronounced three-dimensional (3D) effects, while decay of blast on tank side is rather two-dimensional (2D). The
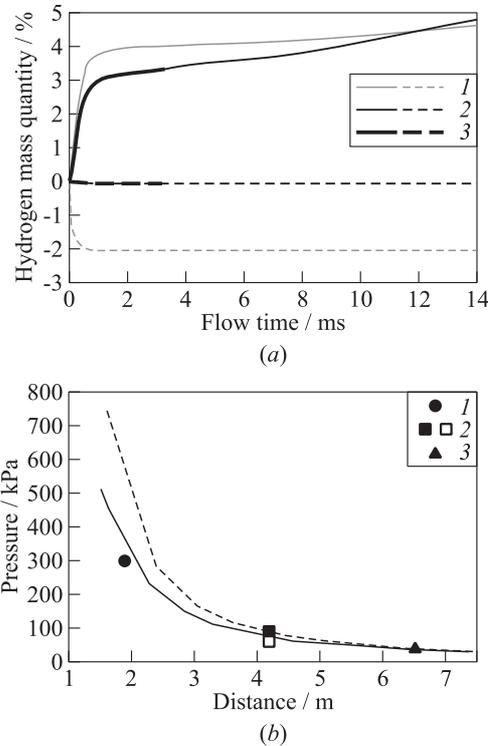
V. V. Molkov et al.

Figure 1 Hydrogen burned mass (solid curves) and numerical "loss" of hydrogen (dashed curves) in simulations as a function of time (*a*) (*1* — CFL = 0.2; *2* — 0.1; and *3* — CFL = 0.05) and maximum pressure as a function of distance from the tank in directions perpendicular to (CFD — dashed curve and experiments — filled signs) and along (CFD — solid curve and experiments — empty signs) the tank axis (*b*) (*1* — 1.9 m; *2* — 4.2; and *3* — 6.5 m)

difference disappears at distance larger than about 6 m. When the blast reached the third sensor at 6.5 m, the amount of burnt hydrogen was 4.3%.

Figure 2 shows experimental (solid lines of different thickness) and simulated (dashed lines) pressure transients for three sensor locations used in the test. Figure 2*a* shows results of simulation in per-
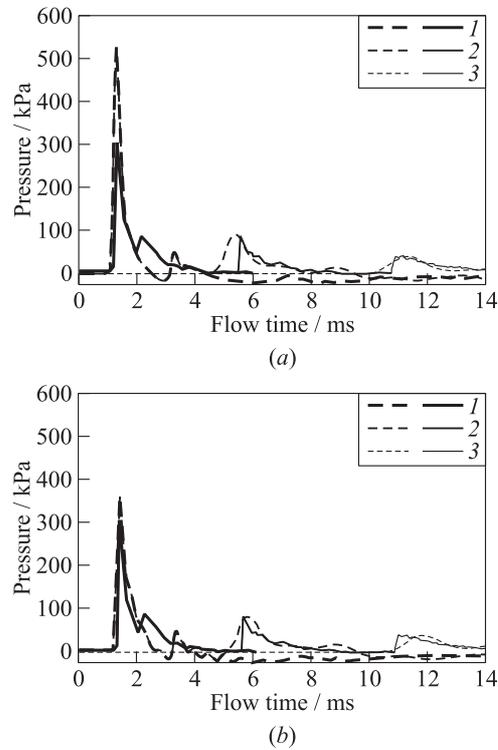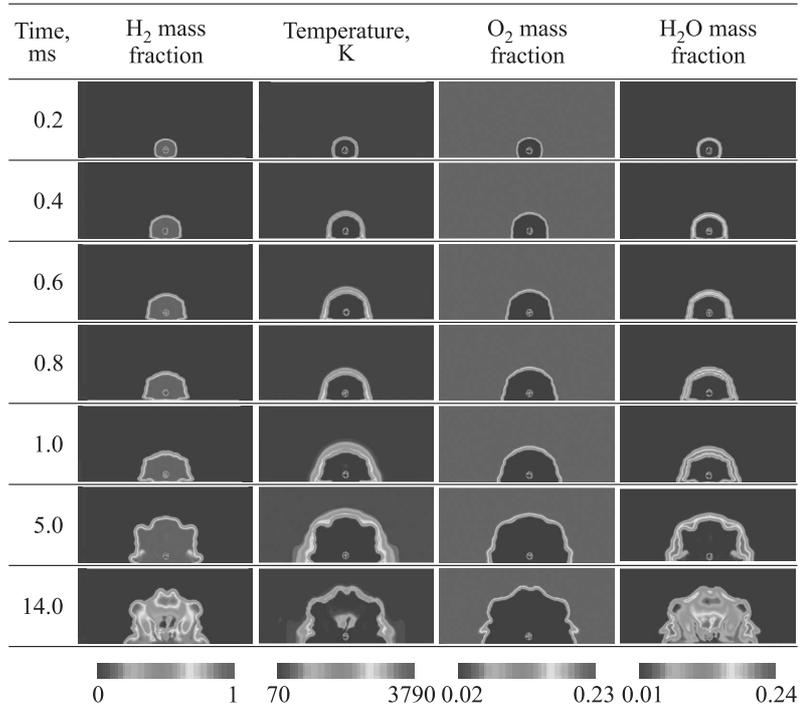
Figure 2 Simulations (dashed curves) vs. the USA test pressure transients (solid curves): (*a*) experimental vs. simulated pressures in direction perpendicular to the tank axis; and (*b*) experimental pressures in direction perpendicular to the tank axis vs. simulated pressures in direction along the tank axis; *1* — 1.9 m; *2* — 4.2; and *3* — 6.5 m

pendicular to the tank axis direction, and Fig. 2*b* in direction along the tank axis. There is deviation between simulations and experiment in the nearfield, which practically disappears for sensors located at 4.2 and 6.5 m.

Fireball dynamics is shown in Table 1 by snapshots of hydrogen mass fraction, temperature, and mass fractions of oxygen and water vapor at time from 0.2 to 14 ms.

Table 1 Fireball dynamics. (Refer color plate, p. XXX.)

Time, ms	H_2 mass fraction	Temperature, K	O_2 mass fraction	H_2O mass fraction
0.2				
0.4				
0.6				
0.8				
1.0				
5.0				
14.0				

0	1	70	3790	0.02	0.23	0.01	0.24

Japanese tests

The CFL sensitivity test is conducted to assure the solution convergence. The solution convergence was analyzed by using change in pressure transients (shown in Fig. 3 for CFL from 0.6 to 0.02) and by controlling amount of burned hydrogen and imbalance of hydrogen in simulations (numerical "loss"). A slight increase of burnt hydrogen was observed for CFL = 0.2 (about 0.04%) compared to the solutions with lower CFL = 0.1. To reduce simulation time by factor of two, the CFL = 0.2 was used in the rest of simulations.

About 10% higher pressure peak was observed for CFL = 2 at 2 ms (not shown in Fig. 3). However, deviation decreases with
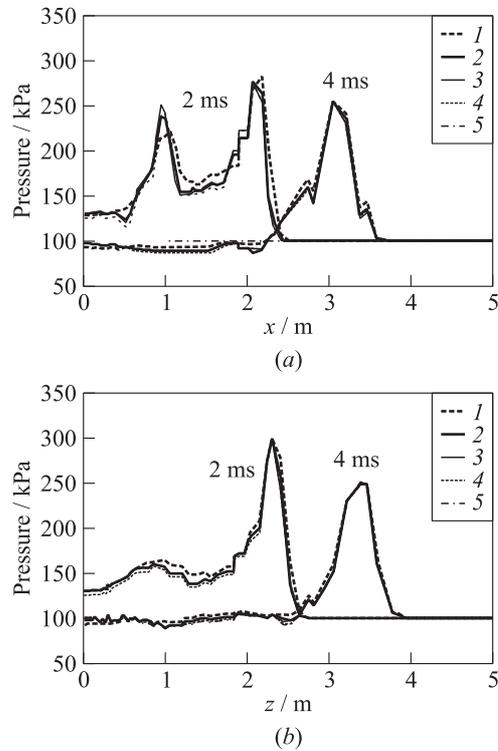
V. V. Molkov et al. **267**

Figure 3 The CFL convergence test: pressure distribution in x (along tank axis) (a) and z (perpendicular to the tank axis) directions (b) at 2 and 4 ms (Japanese Test 1): 1 — CFL = 0.6; 2 — 0.2; 3 — 0.1; 4 — 0.07; and 5 — CFL = 0.02

time and travelled distance, becoming negligible when the pressure wave reaches the first sensor at 5 m. Burnt hydrogen increased from about 8.7% (CFL = 0.2) to 11% (CFL = 2) at 20 ms. The increase is not great enough to affect the pressure at location of sensors in z direction. Mass imbalance increases for higher CFLs, but it maintains below 0.5%.

Figure 4 shows the comparison between the experimental and simulated pressure transients for Tests 1 and 2. The simulation with
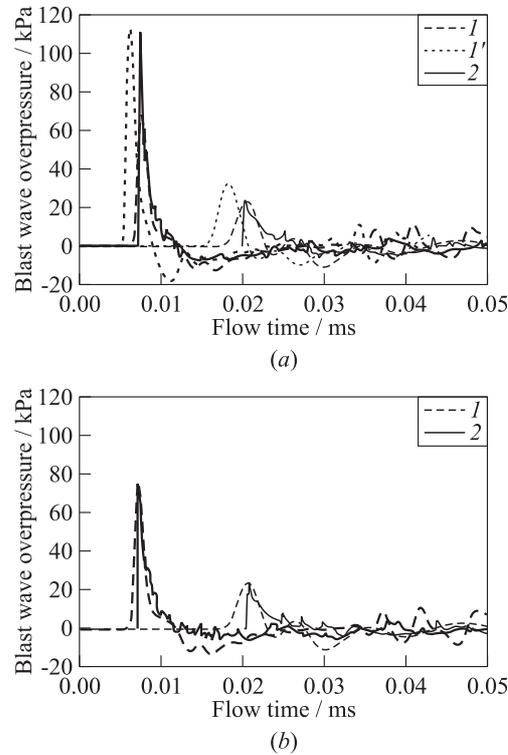
268   *V. V. Molkov et al.*

Figure 4 Simulated (*1* and *1'*) vs. experimental (*2*) pressure dynamics at 5- and 10-meter sensor locations: (*a*) Test 1, including effect of half tank rupture (*1'*); and (*b*) Test 2

instantaneous tank opening underestimates pressure at 5 m and re-produces pressure at 10 m. Negative pressure phase is well repro-duced in time and magnitude. In the case of only half tank opening (in direction of sensors), pressure at 5 m is reproduced in magni-tude but appears earlier, and the negative phase amplitude is a bit high.

As shown in Fig. 5, more than 5% of hydrogen burns within 1 ms. The higher rate of combustion could be because of the high pres-sure at contact surface and high temperature of compressed air due
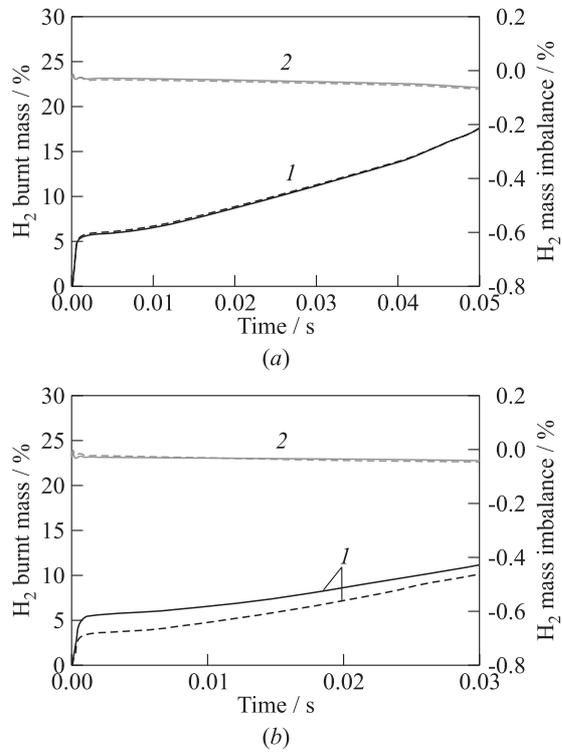
V. V. Molkov et al. **269**

Figure 5 Burnt hydrogen (*1*) and hydrogen mass imbalance (*2*) for Test 1 (solid curve) and Test 2 (dashed line) (*a*); and grid sensitivity (solid curves — course grid and dashed curves — fine grid) for Test 1 (CFL = 0.1) (*b*)

to the blast wave compression, stronger mixing during acceleration of lighter gas to heavier gas (Rayleigh–Taylor instability, see snapshots above), and dilution of combustion at contact surface by water vapor at later stages. The possible contribution of numerics to this strong reduction of combustion rate after about 1 ms has to be yet clarified.

When the sensor at 10 m is reached, the burnt hydrogen achieves 8.7%. The mass balance is shown to be under control and

V. V. Molkov et al.

below 0.1% up to 50 ms. The overpressure peak at 5 m for Test 1 is believed to depend not only on stored mechanical energy and initial release of chemical energy during combustion, but on unknown dynamics of the tank rupture. The effect of burner presence below the bursting tank, fire surrounding the tank, and presence of fragments through tank segmentation were individually investigated. Pressure dynamics at sensors was not significantly affected, whereas burnt hydrogen presented a slight increase, albeit contained within +1.3%.

Another studied numerical scenario was the tank rupture in two pieces with size of half of the tank. This scenario is supported by experimental observations by Zalosh [7] and Pittman [15]. The external surface of the tank was cut along the cylinder axis in two equal portions. The part in the direction of sensors was removed at the start of the calculation, while the second half was removed with delay of about 0.7 ms.

Figure 4*a* shows the effect of opening of solely half of the tank on overpressure at the two sensors. As a result, the pressure increased by 40% at 5 m, reproducing the experimental peak. At the same time, a noticeable 30 percent increase is observed for simulated pressure at 10 m. No significant difference was observed in the quantity of burnt hydrogen between the two simulated cases.

Test 2 pressure dynamics is shown in Fig. 4*b*. Pressure peaks are well reproduced, as well as the overall dynamics during the shown 50 ms. As expected, burnt hydrogen is not different from Test 1 (see Fig. 5). Mass imbalance is below 0.1% and it follows the same trend as in Test 1. The time required by the simulation of 50 ms was approximately 40 h on a 32-processor machine. Time step at constant CFL = 0.2 increased from 1.7 to 5.9 μs.

Results of a grid sensitivity study with CFL = 0.1 are shown in Fig. 5*b*. The length of CVs inside and in the surroundings of the tank and the zone where the sensors are located was halved. The resulting mesh had 723044 CVs. No significant difference is noticed for sensor at 5 m. Sensor at 10 m recorded a lower (about 10%) and slower pressure wave on finer grid. This is thought to be associated with the reduced combustion rate for the finer grid (-2%) as a result of the use of finite-rate combustion submodel. Simulation for finer grid required about 10 days, while less than 2 days were needed for the coarse grid simulation (CFL = 0.1).
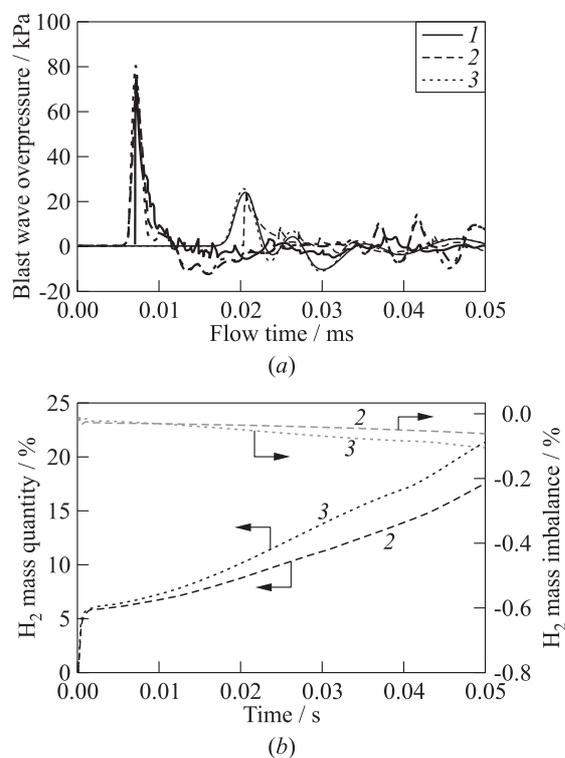
V. V. Molkov et al. **271**

(a)

(b)

Figure 6 Turbulence SGS model sensitivity for Test 2: (a) pressure dynamics; and (b) burned hydrogen and hydrogen mass balance: 1 — experiment; 2 — LES RNG; and 3 — LES Smagorinsky–Lilly

Figure 6 compares LES simulations with use of RNG SGS and Smagorinsky–Lilly SGS turbulence models. The choice of SGS turbulence model influences combustion at later stages, and thus fireball size, and some effect on maximum pressure. The Smagorinsky–Lilly model results in a higher combustion of hydrogen.

Radiation modeling was included in the CFD approach to calculate the thermal hazards in terms of radiative heat flux from the fireball. Neither the pressure dynamics or the burnt hydrogen were affected.

Concluding Remarks

The CFD model is developed to simulate blast wave and fireball dynamics after high-pressure hydrogen tank rupture in a fire. The model allowed to get insight into the process. The contribution of combustion to the blast wave strength is assessed. The convergence of solution is found at CFL number below usually used values of CFL = 0.7–0.9 for deflagrative combustion. The simulations are compared to experimental pressure transients at different distances from the tank. The difference in pressures in directions perpendicular and along the tank axis in the near zone is confirmed. It is concluded that tank opening could affect pressure of the blast wave in a near field but not in a far field.

Acknowledgments

References

1. Dadashzadeh, M., S. Kashkarov, D. Makarov, and V. Molkov. 2018. Risk assessment methodology for onboard hydrogen storage. *Int. J. Hydrogen Energ.* 43(12):6462–6475.

2. Shentsov, V., W. Kim, D. Makarov, and V. Molkov. 2016. Numerical simulations of experimental fireball and blast wave from a high-pressure tank rupture in a fire. *8th Seminar (International) on Fire and Explosion Hazards.* Hefei, China.

3. Kim, W., V. Shentsov, D. Makarov, and V. Molkov. 2017. Simulations of blast wave and fireball occurring due to rupture of high-pressure hydrogen tank. *Safety* 3(2):16.

4. Shentsov, V., D. Makarov, and V. Molkov. 2018. Blast wave after hydrogen storage tank rupture in a tunnel fire. *Symposium (International) on Tunnel Safety and Security*. Borås, Sweden.

5. Weyandt, N. 2005. Analysis of induced catastrophic failure of a 5000 psig Type IV hydrogen cylinder. Southwest Research Institute Report for the Motor Vehicle Fire Research Institute. 01.06939.01.001.

6. Zalosh, R., and N. Weyandt. 2005. Hydrogen fuel tank fire exposure burst test. SAE Paper No. 2005-01–1886.

7. Zalosh, R. 2007. Blast waves and fireballs generated by hydrogen fuel tank rupture during fire exposure. *5th Seminar (International) on Fire and Explosion Hazards*. Edinburgh, U.K.

8. Weyandt, N. 2006. Vehicle bonfire to induce catastrophic failure of a 5000-psig hydrogen cylinder installed on a typical SUV. Southwest Research Institute Report for the Motor Vehicle Fire Research Institute.

9. Molkov, V., and S. Kashkarov. 2015. Blast wave from a high-pressure gas tank rupture in a fire: Stand-alone and under-vehicle hydrogen tanks. *Int. J. Hydrogen Energ.* 40(36):12581–12603.

10. Steiner, H., and W. Gretler. 1994. The propagation of spherical and cylindrical shock waves in real gases. *Phys. Fluids* 6(6):2154–2164.

11. Magnussen, B. F., and B. H. Hjertager. 1977. On mathematical modeling of turbulent combustion with special emphasis on soot formation and combustion. *Symposium (International) on Combustion*. 16(1):719–729.

12. Yakhot, V., and S. Orszag. 1986. Renormalization group analysis of turbulence. I. Basic theory. *J. Sci. Comput.* 1:3–51.

13. Smagorinsky, J. 1963. General circulation experiments with the primitive equations. I. The basic experiment. *Mon. Weather Rev.* 91:99–164.

14. Murthy, J. Y., and S. R. Mathur. 1998. Finite volume method for radiative heat transfer using unstructured meshes. *J. Thermophys. Heat T.* 12(3):313–321.

15. Pittman, J. F., and Naval Surface Weapons Center White Oak Lab Silver Spring MD. 1976. Blast and fragments from superpressure vessel rupture. Defense Technical Information Center. 132 p.